# GRP94 knockdown inhibits proliferation and migration in human cervical cancer cells potentially by downregulating ERK/c-Myc

HANIKEZI TUERXUN, REZIWANGULI AINI, YANXIA CHEN, KA DING and ZUFEIYA AILI

Department of Gynecology, The First Affiliated Hospital of Xinjiang Medical University, Ürümqi, Xinjiang Uyghur Autonomous Region 830054, P.R. China

Received December 15, 2025; Accepted September 16, 2026

DOI: 10.3892/mco.2026.2989

**Abstract.** The endoplasmic reticulum chaperone glucose-regulated protein 94 (GRP94)/gp96, encoded by HSP90B1, supports the folding and trafficking of a set of secreted and membrane proteins that are important for survival, adhesion and proliferation in multiple solid tumors, including breast, lung, esophageal and pancreatic cancers. However, its expression pattern in clinical cervical cancer, as well as its functional contribution to cervical cancer cell proliferation and migration, is not well established. The present study examined the expression of GRP94 in paired tissue samples from 6 patients with cervical cancer using reverse transcription-quantitative PCR, western blotting and immunohistochemistry. GRP94 mRNA and protein levels were significantly upregulated in cancer tissues compared with those in matched adjacent cervical tissues. Consistently, GRP94 was expressed at higher levels in HeLa and SiHa cells than in the non-cancer Ect1 cell line. GRP94 knockdown in HeLa and SiHa cells significantly reduced cell proliferation as assessed by Cell Counting Kit-8 assays, and decreased the fraction of 5-ethynyl-2'-deoxyuridine-positive nuclei. Flow cytometric analysis showed a redistribution of the cell-cycle profile with S-phase accumulation and a corresponding reduction in $G_0/G_1$ distribution in GRP94-knocked down cells, accompanied by decreased cyclin D1 and increased p21 protein expression levels. Furthermore, GRP94 knockdown reduced cell migration by >50% compared with that in control cells, as assessed using Transwell migration assays. At the signaling level, it was found that GRP94 knockdown was associated with reduced expression of c-Myc and extracellular signal-regulated kinase (ERK) protein levels in both HeLa and SiHa cells. However, the phosphorylated-ERK/total ERK ratio was not significantly altered. These findings suggest that GRP94 contributes to the maintenance of proliferative and migratory phenotypes in cervical cancer cells and is associated with changes in ERK and c-Myc protein abundance, although the underlying mechanistic relationships remain to be defined.

*Correspondence to:* Dr Zufeiya Aili, Department of Gynecology, The First Affiliated Hospital of Xinjiang Medical University, 137 South Liyushan Road, Ürümqi, Xinjiang Uyghur Autonomous Region 830054, P.R. China
E-mail: zufeiya18699159658@163.com

*Key words:* glucose-regulated protein 94 (HSP90B1), cervical cancer, proliferation, cell-cycle regulation, ERK/c-Myc

## Introduction

Cervical cancer remains a major global health issue despite advances in vaccination, screening and therapy (1,2). The estimation of the World Health Organization in 2024 suggests that there are ~604,000 new cases of cervical cancer and ~280,000 mortalities worldwide (3), with ~94% of mortalities occurring in low and middle-income countries, showing persistent inequities in prevention and treatment (4). Even where chemoradiation and more recently immunotherapy, such as pembrolizumab, have been integrated into standard regimens (5,6), durable control of advanced disease remains limited, motivating the search for targetable tumor-maintenance mechanisms (7).

Persistent infection with high-risk human papillomavirus (HPV), particularly types 16 and 18, drives oncogenic transformation of cervical epithelial cells through sustained viral oncoprotein expression and dysregulation of protein homeostasis (8). One stress-adaptation system with direct relevance to tumor biology is the endoplasmic reticulum (ER) chaperone network (9). The ER heat shock protein 90 paralog glucose-regulated protein 94 (GRP94; also known as gp96 and encoded by the HSP90B1 gene) is a target-selective chaperone required for the folding and surface expression of a restricted set of secreted and membrane proteins that orchestrate survival, adhesion and innate immunity (10-12). Classical genetic and biochemical studies established that GRP94 is indispensable for the expression of various Toll-like receptors (TLRs), including TLR1/2/4/5/7/9, and for a broad panel of integrins, including α4, αL and β2-containing integrins, thereby coupling tumor and microenvironmental stress to inflammatory signaling and cell-matrix interactions (13-15). Beyond innate immunity and adhesion, GRP94 also chaperones pro-insulin-like growth factor (IGF)-II, a mitogenic hormone whose secretion strictly depends on GRP94 function, linking the chaperone to growth factor availability (16). In the mouse intestinal epithelial tissues, GRP94 is further required for canonical Wnt signaling by enabling the maturation of the co-receptor low-density lipoprotein receptor-related protein 6

(LRP6), situating GRP94 upstream of proliferative transcriptional programs frequently activated in tumors (17). In the setting of HPV infection, chronic activation of the unfolded protein response and ER stress pathways are expected to increase reliance on ER chaperones, including GRP94, to support the stability of viral E6/E7 and host growth-promoting proteins, such as AKT, RAF1, CDK4, CDK6 and Src (18).

Consistent with these relationships, HSP90B1/GRP94 is frequently overexpressed in human tumors, and often associates with aggressive features, including advanced tumor stage, increased metastatic behavior and tumor recurrence, as well as poorer outcomes (11,19). Pan-cancer analyses of gastric, colorectal, lung and esophageal cancer have linked GRP94 overexpression to advanced stage, recurrence or shortened survival (19-21). Importantly for therapeutic tractability, selective pharmacological inhibition of GRP94 by PU-WS13 remodels the tumor microenvironment *in vivo*, reducing M2-like macrophages, increasing $CD8^+$ infiltration and constraining tumor growth in a triple-negative breast cancer model (22), thus supporting the concept that GRP94 is a potential target in solid tumors (21-24).

Regarding cervical cancer, available data are still limited. Previous mechanistic studies showed that higher basal GRP94 levels in cervical carcinoma cell lines (including HeLa) are associated with decreased sensitivity to X-ray-induced cell death, and that small interfering RNA-mediated GRP94 knockdown can sensitize certain cervical cancer cell lines, implicating a role of GRP94 in radioresistance (25,26). However, whether GRP94 is consistently upregulated in clinical cervical tumors, and whether cervical cancer cells depend on GRP94 to sustain proliferative and migratory phenotypes remain insufficiently resolved.

The present study addressed this gap by aligning tissue-level evidence with cell-level mechanisms. The current study aimed to determine whether GRP94 is upregulated in cervical cancer tissues and cell lines, and to evaluate whether loss of GRP94 would affect cell proliferation, cell-cycle progression and migration. To this end, GRP94 expression was examined in clinical specimens. In HeLa and SiHa cell lines, cell proliferation, cell-cycle distribution and migration were evaluated following GRP94 knockdown. Extracellular signal-regulated kinase (ERK) and c-Myc levels were also examined following GRP94 knockdown in the aforementioned cell lines because both signaling pathways are established regulators of cell proliferation and cell-cycle progression (27,28). The aim was to determine whether changes in ERK/c-Myc signaling would be involved in GRP94-dependent regulation of cervical cancer cell proliferation and migration.

## Materials and methods

*Human specimens*. Paired cervical specimens (primary squamous carcinoma tissue and matched control tissue (collected at least 3 cm from the tumor margin) from 6 female patients with cervical cancer undergoing surgery at The First Affiliated Hospital of Xinjiang Medical University (Ürümqi, China) from January 2023 to August 2024 were analyzed in the present study. The patients' age ranged from 45 to 65 years (mean age ± SD, 54.16±8.42), and the cancer stage was confirmed histologically to be IB-IIA according to the International Federation of Gynecology and Obstetrics (29). Eligible patients were women aged ≥18 years who were scheduled to undergo surgery for cervical malignancy or clinically suspected cervical malignancy, had a postoperative pathological diagnosis of cervical malignancy, had sufficient residual tissue available after routine pathological examination, were able to provide informed consent and voluntarily provided written informed consent. For the principal paired-expression analysis, patients who had received neoadjuvant radiotherapy, chemotherapy or other systemic anticancer therapy that could substantially alter tissue molecular expression were excluded. Freshly removed tissues were fixed in 4% paraformaldehyde (PFA) in PBS for 2 h at room temperature, followed by 10-22 h at 4˚C, and then paraffin embedded for histological analysis. In addition, a portion of each tissue was snap-frozen in liquid nitrogen immediately upon surgical removal and maintained at -80˚C until further use. The study protocol was approved by The First Affiliated Hospital of Xinjiang Medical University Ethics Committee (approval no. 24030157). All participants provided written informed consent. Specimen handling, pre-analytic variables and assay reporting followed the Reporting Recommendations for Tumor Marker Prognostic Studies where applicable (30).

*Cell lines and culture*. The human cervical cancer cell lines HeLa (cat. no. HYC3185-2) and SiHa (cat. no. HYC3189), as well as the immortalized cervical epithelial cell line Ect1 (cat. no. BFN60805985), were purchased from Shanghai OBiO Technology (Group) Corp., Ltd. Cells were authenticated by single-nucleotide polymorphism analysis, and all cell lines were routinely tested and confirmed to be mycoplasma-negative. Cells were cultured in DMEM supplemented with 10% FBS (Gibco; Thermo Fisher Scientific, Inc.), 100 U/ml penicillin and 100 $\mu$g/ml streptomycin at 37˚C in a humidified atmosphere with 5% $CO_2$. Experiments were performed using cells within 10-15 passages after thawing.

*GRP94 knockdown by small hairpin RNA (shRNA)*. Plasmids (U6-shRNA-WPRE backbone) encoding a human GRP94-targeting shRNA (shGRP94, 5'-CGTGGTCTGTTT GACGAATAT-3') or a non-targeting shRNA control (shCtrl, 5'-TTCTCCGAACGTGTCACGT-3') were constructed by Shanghai OBiO Technology (Group) Corp., Ltd. The shRNA constructs were sequence-verified by the manufacturer. HeLa and SiHa cells were seeded until reaching 60-70% confluence, and then transfected with 3 $\mu$g plasmid DNA containing either shGRP94 or shCtrl using 9 $\mu$l EZ Trans Cell Transfection Reagent [cat. no. AC04L091; Shanghai OBiO Technology (Group) Corp., Ltd.] according to the manufacturer's protocol. Specifically, the DNA-reagent complexes were incubated for 10-15 min at room temperature before addition to the cells. Cells were then incubated with the transfection complexes at 37˚C in 5% $CO_2$ for 12-16 h, after which the medium was replaced with fresh complete medium. Knockdown efficiency was determined 48-72 h after transfection using western blotting.

*RNA extraction and RT-qPCR*. Total RNA from tissues or cultured cells was extracted with RNAiso Plus (Takara Bio, Inc.), treated with DNase I to remove genomic DNA, and

reverse transcribed into cDNA using HiScript IV All-in-One Ultra RT SuperMix for qPCR (cat. no. R433; Vazyme Biotech Co., Ltd.) following the manufacturer's instructions. RT-qPCR was performed using SupRealQ Purple Universal SYBR qPCR Master Mix (cat. no. Q412; Vazyme Biotech Co., Ltd.) on an Applied Biosystems 7500 Real-Time PCR System (Thermo Fisher Scientific, Inc.). The primer sequences were as follows: GRP94 forward, 5'-GGATGGTCTGGCAACATG GA-3' and reverse, 5'-CCGAAGCGTTGCTGTTTCAA-3'; and GAPDH forward, 5'-GTCTCCTCTGACTTCAACAGC G-3' and reverse, 5'-ACCACCCTGTTGCTGTAGCCAA-3'. The thermocycling conditions were 95˚C for 10 min, followed by 45 cycles of 95˚C for 12 sec, 56˚C for 12 sec and 72˚C for 12 sec. Each biological sample was assayed in technical triplicates. Relative mRNA expression was calculated according to the $2^{-\Delta\Delta Cq}$ method (31) using GAPDH as the reference gene.

*Protein extraction and western blotting*. Cells and frozen tissue samples were lysed in RIPA lysis buffer (Beyotime Biotechnology) supplemented with protease and phosphatase inhibitor cocktails (Beyotime Biotechnology) on ice for 30 min, and clarified by centrifugation at 12,000 x g for 15 min at 4˚C. Protein concentrations were determined using a BCA Protein Assay Kit (Beyotime Biotechnology). Equal amounts of protein (20-40 $\mu$g per lane) were separated by 4-12% (cat. no. P0056; Beyotime Biotechnology) or 4-15% (cat. no. P0465S; Beyotime Biotechnology) precast SDS-PAGE gels and transferred onto PVDF membranes (Immobilon; MilliporeSigma). Membranes were blocked with 5% bovine serum albumin (BSA) in TBS-Tween 20 (TBST; 20 mM Tris-HCl, 150 mM NaCl, 0.1% Tween-20) for 1 h at room temperature and incubated overnight at 4˚C with the following primary antibodies (all from Cell Signaling Technology, Inc. at a 1:1,000 dilution unless otherwise specified): Anti-GRP94 [Grp94 (D6X2Q) rabbit monoclonal antibody (mAb); cat. no. 20292], anti-ERK1/2 [p44/42 MAPK (Erk1/2) antibody; cat. no. 4695], anti-phosphorylated (p)-ERK1/2 [phospho-p44/42 MAPK (Erk1/2) (Thr202/Tyr204); cat. no. 4370], anti-c-Myc (cat. no. 13987), anti-p21 (cat. no. 2947), anti-cyclin D1 [cyclin D1 (92G2) rabbit mAb; cat. no. 2978] and anti-GAPDH (cat. no. 2118). After washing with TBST, the membranes were incubated with an HRP-conjugated secondary antibody (goat anti-rabbit IgG-HRP; 1:5,000; cat. no. AB-6721; Abcam) for 2 h at room temperature. Bands were visualized using Immobilon ECL Ultra Western HRP Substrate (cat. no. WBULS0100; MilliporeSigma) and imaged with a digital gel imaging system. Densitometric analysis was performed using ImageJ software (version 1.54; National Institutes of Health), with protein levels normalized to GAPDH as the loading control. In addition, the p-ERK/ERK ratio was calculated for each biological replicate by dividing the p-ERK signal by the corresponding total ERK signal.

*Immunohistochemistry (IHC)*. PFA-fixed, paraffin-embedded cervical tissue sections (3 $\mu$m) were deparaffinized in xylene, rehydrated through graded ethanol series, and subjected to heat-induced epitope retrieval in 10 mM sodium citrate buffer (pH 6.0) at ~100˚C for 15-20 min. Endogenous peroxidase activity was quenched by incubation in 3% $H_2O_2$ for 10 min, and non-specific binding was blocked with normal goat serum (cat. no. C0265; Beyotime Biotechnology) for 30 min at room temperature. Sections were incubated overnight at 4˚C with a rabbit anti-human GRP94 antibody (1:100; cat. no. 83147-4-PBS; Proteintech Group, Inc.). After washing with PBS, sections were incubated with an HRP-conjugated secondary antibody (1:200; cat. no. AB-6721; Abcam) for 30 min at room temperature and developed with 3,3'-diaminobenzidine (DAB; Beyotime Biotechnology). Nuclei were counterstained with hematoxylin (Beyotime Biotechnology) for 1-2 min at room temperature, and slides were dehydrated, cleared and mounted. Images were acquired using an Olympus BX51 light microscope (Olympus Corporation). DAB staining intensity within the tissue area was quantified in multiple representative microscopic fields from each specimen using ImageJ software (version 1.54), and the mean value was calculated and expressed as relative DAB mean intensity for quantitative comparison. Image acquisition and evaluation were performed by two observers blinded to sample identity.

*Cell viability/proliferation assay*. Cell viability was assessed using the Cell Counting Kit-8 (CCK-8) assay (cat. no. C0038; Beyotime Biotechnology). HeLa and SiHa cells transfected with shGRP94 or shCtrl were seeded in 96-well plates at a density of 2-5x$10^3$ cells/well in 100 $\mu$l complete medium and allowed to adhere overnight. At 24, 48 and 72 h after seeding, 10 $\mu$l CCK-8 reagent was added to each well and incubated for 1 h at 37˚C in 5% $CO_2$. The absorbance at 450 nm was then measured using a microplate reader (Bio-Rad Laboratories, Inc.). Each condition was tested in ≥5 technical replicates per experiment, and each experiment was independently repeated ≥3 times.

*5-Ethynyl-2'-deoxyuridine (EdU) incorporation assay*. DNA synthesis was evaluated using the BeyoClick™ EdU-488 Cell Proliferation Detection Kit (cat. no. C0071S; Beyotime Biotechnology) according to the manufacturer's instructions. Briefly, HeLa and SiHa cells were seeded in 12-well plates on glass coverslips at 5x$10^4$-1x$10^5$ cells/well and cultured for 24-48 h. EdU was then added to the medium to a final concentration of 10 $\mu$M, and cells were incubated for another 2 h at 37˚C in 5% $CO_2$. Cells were then fixed with 4% PFA in PBS for 15 min at room temperature, permeabilized with 0.3% Triton X-100 in PBS for 15 min, and labeled with Alexa Fluor 488 azide for 30 min at room temperature in the dark to detect the incorporated EdU. Nuclei were counterstained with Hoechst 33342 for 10-30 min at room temperature in the dark (supplied in the aforementioned kit) and coverslips were mounted using anti-fade mounting medium. Fluorescence images were captured using an Olympus IX inverted fluorescence microscope (Olympus Corporation) under identical exposure settings. For each condition, EdU-positive and total (Hoechst-positive) nuclei were counted in ≥5 randomly selected fields per sample using ImageJ software (version 1.54; National Institutes of Health). The EdU incorporation rate was expressed as the percentage of EdU-positive nuclei.

*Cell cycle analysis by flow cytometry*. For cell-cycle analysis, shGRP94 and shCtrl-transfected HeLa and SiHa cells were seeded in 6-well plates (2-3x$10^5$ cells/well). To synchronize cells, cultures were serum-starved in 0.5% FBS for 18 h

and then re-stimulated with complete medium containing 10% FBS for 18 h. Next, cells were harvested by trypsinization, washed twice with ice-cold PBS (without $Ca^{2+}$/$Mg^{2+}$, containing 0.5% BSA and 0.1% sodium azide) and fixed in 75% ice-cold ethanol at 4˚C overnight. After washing with PBS, cells were resuspended in PBS containing RNase A (40 $\mu$g/ml) and propidium iodide (PI; 40 $\mu$g/ml), and incubated for 30 min at room temperature in the dark. The DNA content was then analyzed on a BD FACSCelesta™ flow cytometer (Waters Biosciences). Doublets were excluded based on pulse geometry (32), and cell-cycle distributions were determined using FlowJo™ software (version 10.0; Waters Biosciences) with the pragmatic model of Watson *et al* (33).

*Transwell migration assay*. Cell migration was assessed using 24-well Transwell chambers with 8-$\mu$m pore size polycarbonate membranes (Falcon; Corning Life Sciences). The lower chambers were filled with 1 ml complete medium containing 10% FBS as chemoattractant. HeLa and SiHa cells were resuspended in serum-free medium, and $1x10^5$ cells in 500 $\mu$l were added to the upper chamber of each insert. After incubation for 24-48 h at 37˚C in 5% $CO_2$, non-migrated cells on the upper surface of the membrane were gently removed with a cotton swab. The cells that migrated to the lower surface were fixed in 100% methanol for 10 min at room temperature, stained with 0.1% crystal violet for 20-30 min at room temperature, washed with PBS and air-dried. Membranes were imaged under a light microscope (10X objective; Olympus IX), and migrated cells were counted in ≥5 random fields per insert using ImageJ software (version 1.54; National Institutes of Health). Each condition was assayed in triplicate inserts, and experiments were repeated ≥3 times independently.

*Public database survival analysis*. Exploratory survival analysis was performed using the Kaplan-Meier Plotter pan-cancer RNA-sequencing platform (kmplot.com). The cervical cancer cohort was selected, and HSP90B1 was used as the gene symbol for GRP94. Patients were stratified into HSP90B1-high and HSP90B1-low groups according to the median expression cut-off. Overall survival was selected as the endpoint, and survival differences were assessed using the log-rank test. The analysis was performed as an exploratory public database assessment and was not used as primary evidence for the clinical relevance of GRP94.

*Statistical analysis*. All quantitative data are presented as the mean ± SEM. Statistical analyses were performed using GraphPad Prism 10 (Dotmatics). Comparisons between data obtained from the paired cervical specimens were performed using paired Student's t-tests, while comparisons between two unpaired groups were performed using two-tailed, unpaired Student's t-tests. For comparisons among multiple groups, one-way or two-way ANOVA followed by Bonferroni's post-hoc test was applied where appropriate. Normality and homogeneity of variance were verified using the quantile-quantile plot and Brown-Forsythe test, respectively, in GraphPad Prism 10 before applying parametric tests. $P<0.05$ was considered to indicate a statistically significant difference.

## Results

*GRP94 is upregulated in cervical cancer tissues and cell lines, and can be efficiently knocked down by shRNA*. Western blot analysis of paired cervical cancer tissues and adjacent non-cancer tissues showed a consistent upregulation of GRP94 protein expression in tumor samples (Fig. 1A). Semi-quantification across all patients demonstrated a ~50% increase in GRP94 protein expression in tumor tissue compared with that in matched non-cancer cervical tissue ($P<0.01$; Fig. 1D). GRP94 mRNA expression measured by RT-qPCR revealed a similar pattern, with significantly higher transcript levels in tumor tissues ($P<0.01$; Fig. 1C). IHC further confirmed this upregulation, as cervical cancer epithelia exhibited strong and diffuse cytoplasmic GRP94 staining, whereas adjacent non-cancer tissues displayed weak or focal positivity (Fig. 1F). Quantification of DAB staining intensity demonstrated a significant increase in GRP94 expression in the tumor sections ($P<0.01$; Fig. 1E).

Next, the present study examined GRP94 expression in cervical cell lines. GRP94 protein abundance was markedly higher in HeLa cells compared with that in the immortalized cervical epithelial line Ect1 (Fig. 1B). A statistically significant difference in the GRP94 level between SiHa and Ect1 cells was also observed, although the increase was not as evident. To enable loss-of-function studies, GRP94 knockdown was performed in both cancer cell lines with a GRP94-targeting shRNA. Western blotting showed a ~70% reduction in GRP94 protein levels compared with those in the non-targeting shCtrl group ($P<0.001$; Fig. 1G). These results indicate that GRP94 is consistently upregulated in human cervical cancer tissue and cell lines, and can be effectively knocked down.

*GRP94 knockdown reduces the proliferation of HeLa and SiHa cells*. Whether GRP94 contributes to cervical cancer cell proliferation was assessed in HeLa and SiHa cells after knockdown. In both cell lines, CCK-8 assays demonstrated significantly slower proliferation in shGRP94 cultures over time (Fig. 2C and F). The optical density at 450 nm readings in shGRP94 cells remained less than half of that in shCtrl cultures throughout the assay. Two-way ANOVA for both cell lines revealed a significant main effect of time (HeLa: $F_{2,42}=337.2$, $P<0.01$; SiHa: $F_{2,42}=216.3$, $P<0.01$), treatment (HeLa: $F_{1,42}=442.9$, $P<0.01$; SiHa: $F_{1,42}=293.2$, $P<0.01$) and interaction (HeLa: $F_{2,42}=36.75$, $P<0.01$; SiHa: $F_{2,42}=27.59$, $P<0.01$). Post-hoc tests confirmed a sustained reduction in cell viability in the shGRP94 group at 48 and 72 h ($P<0.01$ vs. shCtrl).

Consistent with these findings, EdU incorporation assays revealed that the proportion of EdU-positive nuclei in shGRP94 cells was reduced to <50% of that in shCtrl cultures ($P<0.01$; Fig. 2A, B, D and E), demonstrating a marked decrease in DNA synthesis following GRP94 depletion.

*GRP94 knockdown alters the cell-cycle distribution and the expression of key cell-cycle regulators*. To determine whether reduced proliferation was associated with cell-cycle alterations, PI-based flow cytometry was performed. GRP94 knockdown induced a pronounced redistribution of cell-cycle phases in both HeLa and SiHa cells. Statistical analysis revealed

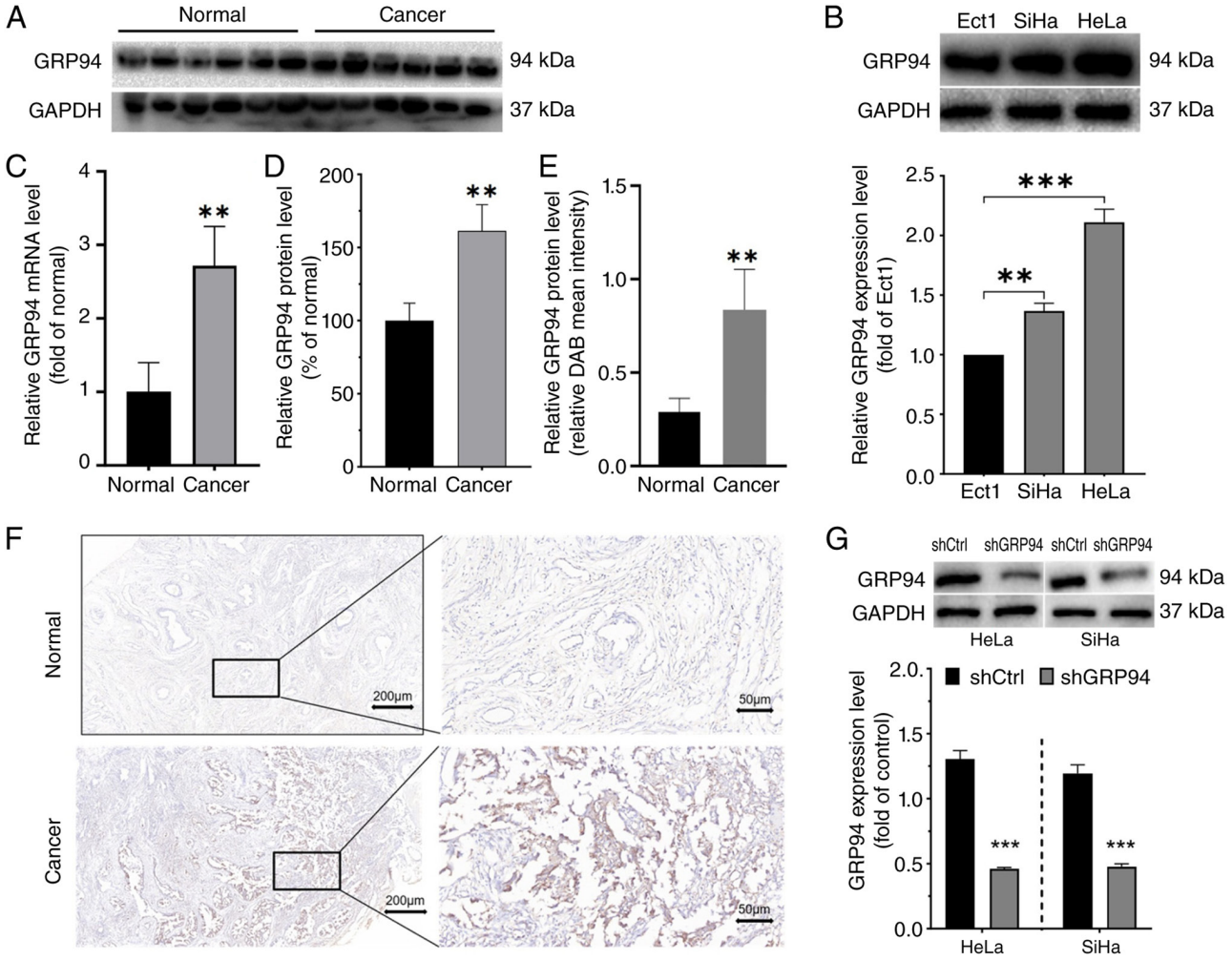



Figure 1. GRP94 is upregulated in human cervical cancer tissues and cell lines. (A) Representative western blots of GRP94 and GAPDH in paired cervical cancer tissues and adjacent non-cancer cervical tissues from 6 patients. (B) Basal GRP94 protein expression in immortalized normal cervical epithelial cells (Ect1) and cervical cancer cell lines (SiHa and HeLa), as determined by western blotting. Quantification of (C) GRP94 mRNA expression and (D) GRP94 protein expression in the paired samples corresponding to panel A. (E) Semi-quantitative analysis of GRP94 IHC staining from the cohort corresponding to panel F. (F) Representative IHC staining of GRP94 in cervical cancer and adjacent non-cancer tissues, showing stronger cytoplasmic staining in tumor epithelium. (G) Validation of GRP94 knockdown efficiency in HeLa and SiHa cells transfected with shCtrl or shGRP94. Data are presented as the mean ± SEM. $^{**}$P<0.01 and $^{***}$P<0.001 vs. non-cancer control or shCtrl. GRP94, glucose-regulated protein 94; Ctrl, control; IHC, immunohistochemistry; sh, small hairpin; DAB, 3,3'-diaminobenzidine.

significant main effects of phase (HeLa: $F_{2,18}$=769.6, P<0.01; SiHa: $F_{2,18}$=1,642, P<0.01) and a significant interaction of phase with treatment (HeLa: $F_{2,18}$=503.6, P<0.01; SiHa: $F_{2,18}$=906.4, P<0.01). Post-hoc tests confirmed that, in both cell lines, the $G_0/G_1$ fraction in the shGRP94 group was reduced by >50% compared with that of the shCtrl group (P<0.01), whereas the S-phase fraction nearly doubled (P<0.01 for phase-matched comparisons) (Fig. 3A, B, D and E). These observations indicate that GRP94 supports normal $G_1$/S transition and/or S-phase progression, and its depletion results in S-phase accumulation.

Subsequently, the expression of key regulators governing the $G_1$/S checkpoint was examined. Western blotting revealed increased levels of the cyclin-dependent kinase inhibitor p21 in both HeLa and SiHa cells following GRP94 knockdown (Fig. 3C). The increase was statistically significant in HeLa cells (P<0.05), whereas SiHa cells exhibited the same trend but did not reach statistical significance due to variability in the shCtrl group. Cyclin D1 abundance was reduced in both cell lines, with the decrease reaching statistical significance in SiHa cells and showing a near-significant trend in HeLa cells (P=0.054). Collectively, the upregulation of p21 coupled with reduced cyclin D1 levels is consistent with impaired $G_1$/S progression and aligns with the observed S-phase accumulation (33).

*GRP94 knockdown impairs the migration of cervical cancer cells*. To assess the role of GRP94 in cell motility, Transwell migration assays were performed. In HeLa cultures, markedly fewer shGRP94 cells migrated through the membrane compared with shCtrl cells, and SiHa cells demonstrated a similar reduction in migratory capacity (Fig. 4A and B). Data summarized from three independent experiments (Fig. 4C) showed that GRP94 knockdown significantly impaired migration in both cervical cancer cell lines (P<0.001), suggesting that GRP94 contributes to both proliferative and migratory phenotypes.

*GRP94 knockdown attenuates ERK/c-Myc abundance*. Since ERK (27) and c-Myc (28) are established regulators of cell

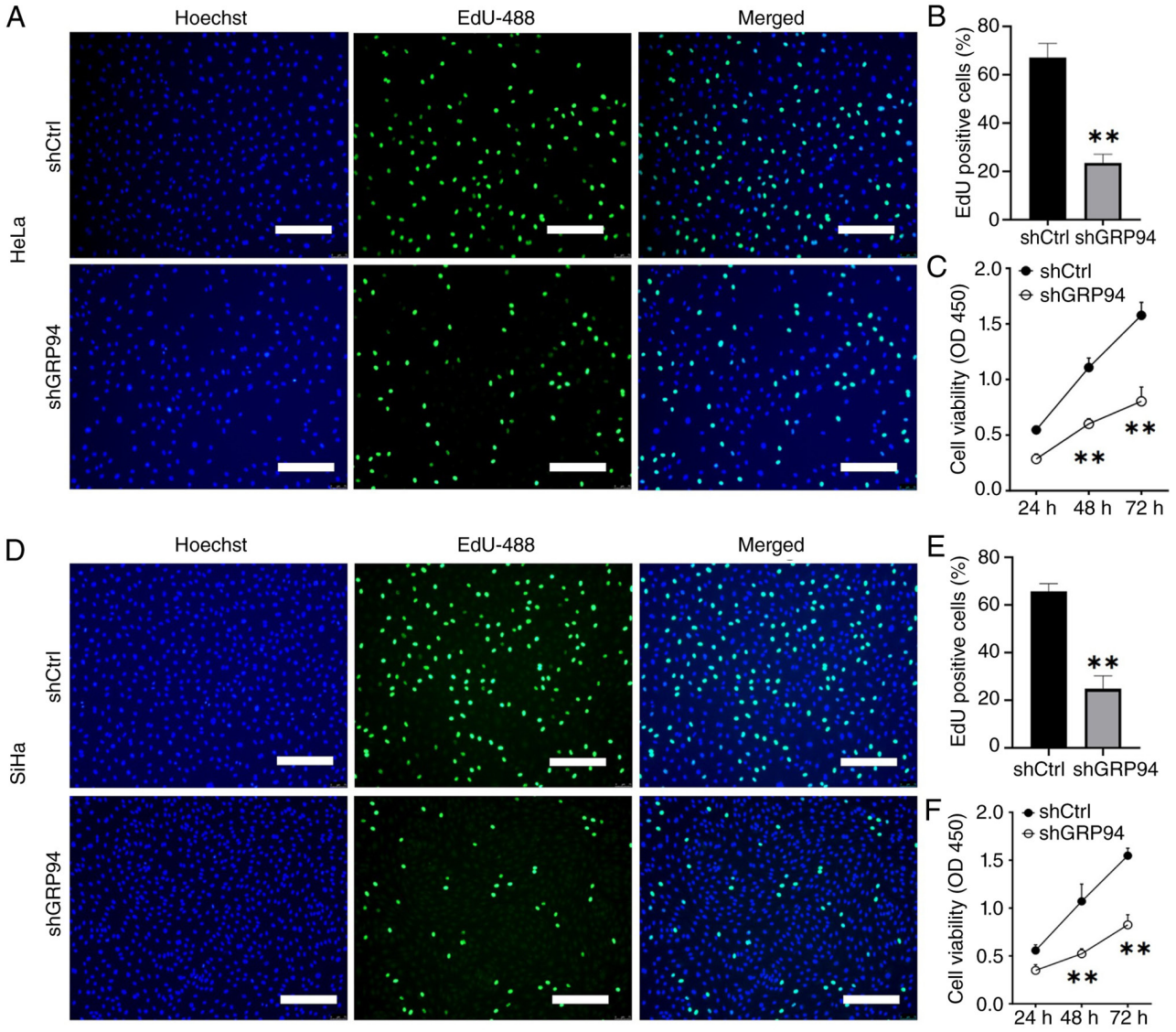



Figure 2. GRP94 knockdown reduces the proliferation of cervical cancer cells. HeLa and SiHa cells expressing shCtrl or shGRP94 were subjected to EdU incorporation and CCK-8 assays. (A) Representative fluorescence images of HeLa cells showing nuclei (Hoechst), proliferating cells (EdU-488) and merged channels. Scale bar, 200 $\mu$m. (B) Quantification of EdU-positive HeLa cells expressed as the percentage of EdU-488-positive nuclei over total Hoechst-stained nuclei. (C) Time course of cell viability measured using the CCK-8 assay ($OD_{450\ nm}$) in shCtrl and shGRP94 HeLa cells. (D) Representative Hoechst/EdU-488/merged images of SiHa cells expressing shCtrl or shGRP94. (E) Percentage of EdU-positive SiHa cells. (F) Time course of cell viability ($OD_{450\ nm}$) in shCtrl and shGRP94 SiHa cells. Data are presented as the mean ± SEM from three independent experiments. Statistically significant differences were assessed using unpaired Student's t-tests or two-way ANOVA with Bonferroni's post-hoc tests where appropriate. $^{**}$P<0.01 vs. shCtrl. GRP94, glucose-regulated protein 94; Ctrl, control; sh, small hairpin; EdU, 5-ethynyl-2'-deoxyuridine; CCK-8, Cell Counting Kit-8; OD, optical density.

proliferation and survival, the present study examined their status after GRP94 knockdown. In both HeLa and SiHa cells, c-Myc protein levels were substantially reduced in the shGRP94 group (P<0.01; Fig. 5A and B). The levels of ERK and p-ERK in the shGRP94 group were also decreased compared with those in the control group (P<0.01; Fig. 5A, C and D). However, no significant changes were observed in the p-ERK/ERK ratio in GRP94-deficient cells (Fig. 5E). These findings suggest that GRP94 may sustain cervical cancer cell proliferation and migration at least in part by supporting ERK and c-Myc expression.

*Higher HSP90B1 expression shows a trend toward poorer survival*. To further explore the clinical relevance of GRP94/HSP90B1, an exploratory Kaplan-Meier analysis was performed using a public cervical cancer RNA-sequencing cohort. Patients were stratified into HSP90B1-high and HSP90B1-low groups using the median expression cut-off level. A trend toward poorer overall survival was observed in the HSP90B1-high group [hazard ratio=1.54 (95% CI, 0.96-2.46); log-rank P=0.073; Fig. S1], which, however, did not reach statistical significance.

## Discussion

In the present study, it was first verified in paired clinical samples from 6 patients with cervical cancer that GRP94 is elevated in cervical cancer specimens compared with adjacent non-cancerous cervical tissue. Consistent with this, GRP94 knockdown in HeLa and SiHa cells reduced cell proliferation,

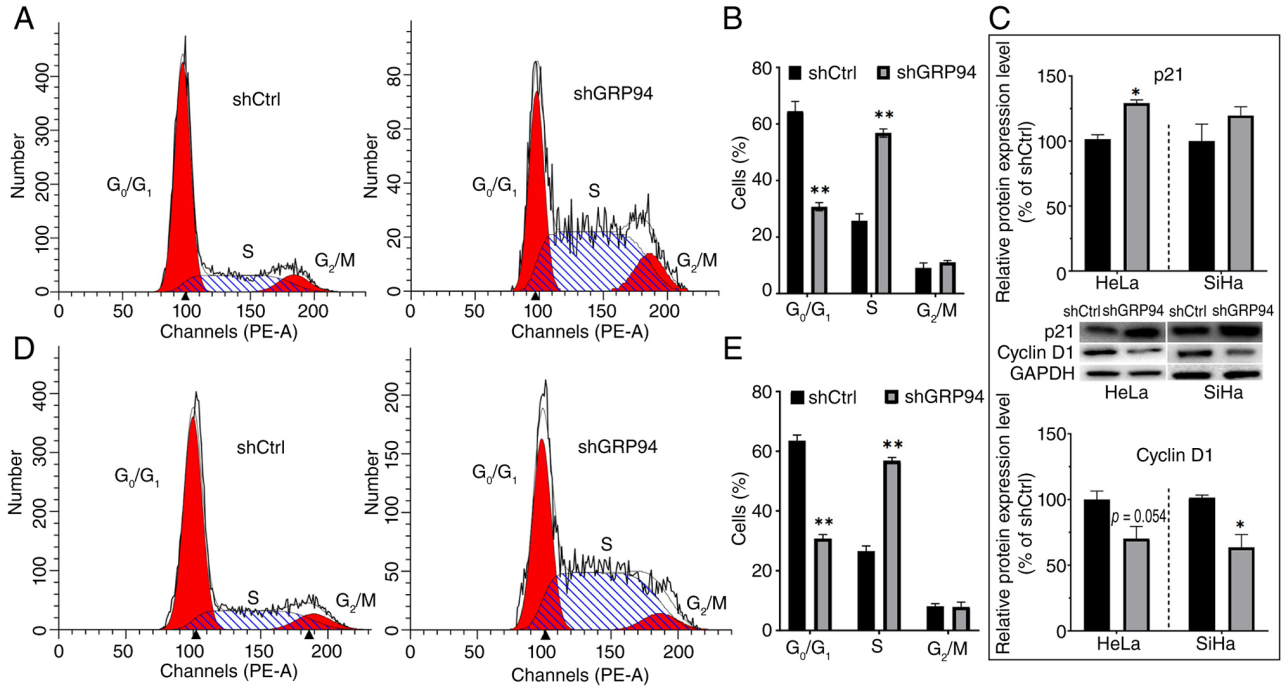



Figure 3. GRP94 knockdown alters cell-cycle distribution and cell-cycle regulators in cervical cancer cells. Cell cycle analysis of HeLa and SiHa cells expressing shCtrl or shGRP94. Cells were fixed in ethanol, stained with propidium iodide and analyzed by flow cytometry. (A) Representative DNA content histograms showing the distribution of HeLa cells in $G_0/G_1$, S and $G_2/M$ phases for the shCtrl and shGRP94 groups. (B) Summary of the percentages of HeLa cells in each cell-cycle phase from three independent experiments. (C) Western blot analysis of p21 and cyclin D1 in HeLa and SiHa cells expressing shCtrl or shGRP94, with GAPDH as a loading control. Representative bands are shown between the two bar graphs. The upper bar graph shows densitometric quantification of p21, while the lower bar graph shows densitometric quantification of cyclin D1, normalized to GAPDH and expressed relative to shCtrl. (D) Representative DNA histograms for SiHa cells. (E) Quantification of the percentages of SiHa cells in $G_0/G_1$, S and $G_2/M$ phases. Data are presented as the mean ± SEM from three independent experiments. Statistically significant differences were assessed using two-way ANOVA with Bonferroni's post-hoc tests or unpaired Student's t-tests as applicable. $^{*}P<0.05$ and $^{**}P<0.01$ vs. shCtrl. GRP94, glucose-regulated protein 94; Ctrl, control; sh, small hairpin.

shifted the cell-cycle distribution toward S-phase accumulation, and attenuated cell migration. Mechanistically, these phenotypes coincided with decreased ERK, p-ERK and reduced c-Myc abundance. The present results are in line with previous studies showing that GRP94 depletion is associated with reduced MAPK-related signaling and impaired proliferative or metastatic phenotypes in tumor models (34,35), while ERK-dependent regulation has been shown to influence c-Myc protein stability and abundance (36,37). Taken together, these results indicated that GRP94 functions as an upstream mediator of cell proliferation and migration programs in cervical cancer models, with ERK/c-Myc serving as a potential readout of its downstream impact (27,28).

The present paired-tissue design minimized inter-individual variability and revealed that GRP94 is upregulated in malignant tissues, which is in line with previous reports of HSP90B1/GRP94 overexpression in multiple solid tumors including breast (23), lung (21,38), esophageal (19,39,40) and pancreatic cancers (41). In cervical cancer models, a similar pattern was also observed at the cell line level, where both HeLa and SiHa cells exhibited higher GRP94 expression relative to that of non-malignant controls (26). As aforementioned, GRP94 facilitates the folding and trafficking of integrins, TLRs, pro-IGF-II and the Wnt co-receptor LRP6, which are involved in signaling pathways important for survival, adhesion and proliferation (14-17). The elevation of GRP94 in cervical cancer tissues may be a result of stress adaptation that favors tumor growth and stress resistance. In the current preliminary study, sufficient samples were not obtained to stratify tissues by clinical covariates (such as stage or HPV genotype), but the consistent upregulation of GRP94 in malignant tissues provided the rationale for evaluating whether cervical cancer cells functionally depend on GRP94 to maintain proliferative and migratory traits. At present, analysis of the publicly available cervical cancer cohort in the KM Plotter pan-cancer RNA-seq database does not provide a clear basis for concluding that HSP90B1/GRP94 has prognostic value, and the cervical cancer-specific literature remains limited in this regard. Thus, to the best of our knowledge, the present study provided initial direct evidence that GRP94 is upregulated in human cervical cancer specimens, while its relationship with prognosis, clinicopathological features and patient outcomes remains to be defined in larger clinically annotated cohorts.

In the present study, it was observed that GRP94 knockdown led to the suppression of cell proliferation in HeLa and SiHa cells. This is broadly in line with prior studies showing that GRP94 overexpression in various solid tumors is associated with aggressive behavior, and that GRP94 knockdown generally reduces cancer cell proliferation and viability. For example, GRP94 depletion in colorectal and endometrial cancer cells reduced proliferation and tumorigenicity *in vitro* and in xenograft models (34,42), and similar effects have been reported in lung and esophageal cancer cell lines (21,40). Notably, it has been shown in the liver tissue that chronic GRP94 deletion induced hyperproliferation of liver progenitor cells, while combined depletion of GRP94 and the tumor

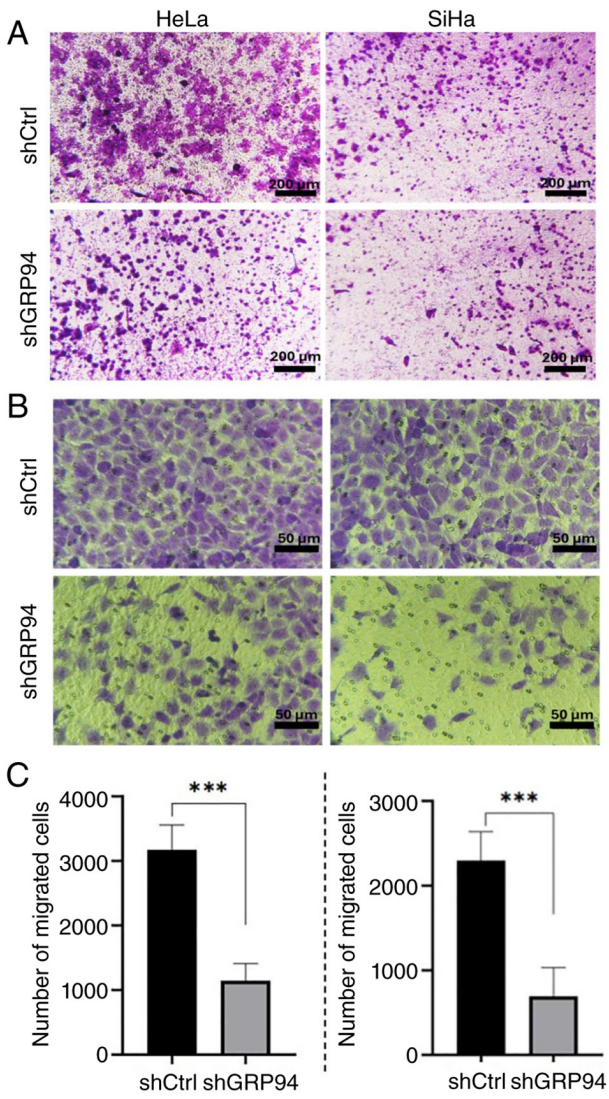



Figure 4. GRP94 knockdown impairs the migration of cervical cancer cells. Representative images of (A) low- and (B) high-magnification of Transwell migration assays in HeLa (left column) and SiHa (right column) cells transfected with shCtrl or shGRP94. Scale bar, 200 $\mu$m (A) or 50 $\mu$m (B). (C) Quantification of migrated cells per field in HeLa and SiHa cultures. Data are presented as the mean ± SEM from three independent experiments and were analyzed using unpaired Student's t-tests. ***P<0.001 vs. shCtrl. GRP94, glucose-regulated protein 94; Ctrl, control; sh, small hairpin.

suppressor PTEN accelerated the development of hepatocellular carcinoma and cholangiocarcinoma, suggesting that the effect of GRP94 loss on cell proliferation and tumorigenesis may be context dependent (43). However, the current study supports the view that, in established carcinoma cells and human cervical cancer tissues, GRP94 behaves predominantly as a classical oncogenic chaperone, and acute suppression of its protein level restrains cell proliferation.

The tumor growth-suppressive effect of GRP94 knockdown coincided with a S-phase accumulation that suggested a restraint in DNA synthesis or S-phase progression rather than a simple $G_1$ arrest. The decrease in cyclin D1 levels together with the increase in p21 levels is consistent with the engagement of a cell-cycle checkpoint. This pattern is in line with the known role of c-Myc in coordinating cyclin D1, cyclin E and p21 to drive $G_1$/S progression (28), as well as with the present observation that GRP94 knockdown lowered ERK and c-Myc abundance. An alternative interpretation of the present results is that GRP94 knockdown induces ER stress and proteostatic imbalance (44), and that this stress response secondarily slows the cell cycle. Limited by the scope of the current study, the current dataset cannot fully distinguish between direct regulation of cell-cycle machinery via ERK/c-Myc and stress-driven checkpoint activation. In addition, the present study did not directly assess apoptosis. Therefore, although the observed reduction in growth is consistent with impaired cell-cycle progression, the current data do not exclude the possibility that increased apoptosis may also contribute to this phenotype. Additional experiments, such as transient c-Myc overexpression or constitutive ERK activation in GRP94-deficient cells, will be important to clarify whether the S-phase phenotype primarily reflects alteration of ERK/c-Myc signaling, a generalized stress program or a combination of both.

GRP94 has been implicated not only in tumor growth control but also in invasion and metastasis, as integrins and other adhesion-related proteins are its targets. It has been reported in colorectal (34), hepatocellular (35), breast (23) and endometrial (42) cancer that GRP94 overexpression is associated with metastatic progression, and that GRP94 knockdown or inhibition reduces migration and invasion *in vitro* and limits metastatic spread *in vivo*. The current finding that GRP94 knockdown in HeLa and SiHa cells reduced cell migration by >50% is consistent with the aforementioned studies, and extends to cervical cancer models, where the effect of GRP94 on cell migration has not been systematically examined to date.

A key interpretive issue is whether the migration deficit simply mirrors reduced proliferation or reflects a more direct role for GRP94 in migration. Reduced migration can be secondary to cytostasis, and the present data do not allow these possibilities to be clearly distinguished, particularly because the EdU incorporation and Transwell migration assays were performed over comparable culture periods. Nevertheless, a previous study has suggested a direct role of GRP94 in cell motility, as GRP94 knockdown has been reported to disrupt intracellular trafficking of F-actin and integrins, including integrin α2 and αL, to impair cell adhesion, polarity and migration (45). Another study has linked GRP94 to epithelial-mesenchymal transition-related transcriptional programs and MAPK-dependent motility (34). Notably, whether similar mechanisms contribute to the migration phenotype observed in cervical cancer cells remains hypothetical and should be examined directly in future studies.

Within this context, the ERK/c-Myc changes observed in the current study may support a potential association between GRP94 status and both cell proliferation and migration. GRP94 supports multiple secreted and membrane proteins that signal through MAPK pathways, including IGF-II/IGF receptors and several integrins (15,16,46), and GRP94 depletion in other tumor types, such as esophageal squamous cell carcinoma and colorectal cancer cells, has been shown to disrupt the ERK pathway and downstream proliferative signaling (34). The ERK-dependent phosphorylation of c-Myc at Ser62 stabilizes the protein, whereas MEK/ERK inhibition or loss of Ser62 phosphorylation

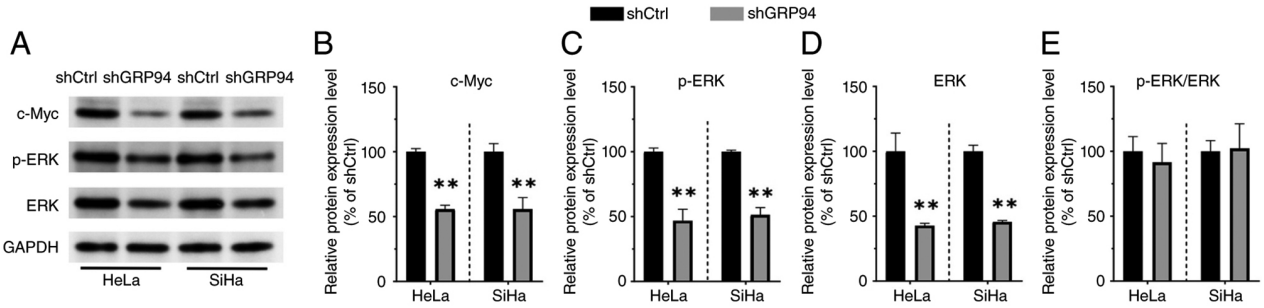



Figure 5. GRP94 knockdown attenuates ERK/c-Myc protein expression in cervical cancer cells. (A) Representative western blots of c-Myc, p-ERK (p-ERK1/2, Thr202/Tyr204), total ERK and GAPDH in HeLa and SiHa cells expressing shCtrl or shGRP94. In the current samples, the lower band of p-ERK1/2 was substantially weaker than the upper bands. In the total ERK blots, the lower band was mostly undetectable as it was noted that the relative intensities of the two ERK1/2 bands can vary according to cell context and immunoblotting conditions. Densitometric quantification of (B) c-Myc, (C) p-ERK (normalized to GAPDH), (D) total ERK (normalized to GAPDH) and (E) p-ERK/ERK ratio, expressed relative to the shCtrl group. Data are presented as the mean ± SEM from three independent experiments. Statistically significant differences were assessed using unpaired Student's t-tests. $^{**}$P<0.01 vs. shCtrl. GRP94, glucose-regulated protein 94; Ctrl, control; sh, small hairpin; p-, phosphorylated.

triggers c-Myc downregulation and $G_1$/S defects (36,37). Given that c-Myc drives the expression of cyclin D1, cyclin E and S-phase genes (28), the parallel decrease in p-ERK and c-Myc observed in the current study provides a possible explanation for the S-phase accumulation and cyclin D1 decrease/p21 increase in GRP94-deficient cells, and may contribute to reduced cell migration through downstream effects on cytoskeletal and adhesion signaling pathways. The novelty of the present study is the explicit demonstration that acute GRP94 loss in cervical cancer cells is sufficient to decrease ERK/c-Myc protein levels in parallel with reduced proliferation and migration.

The present data do not establish ERK/c-Myc as the only or dominant route through which GRP94 supports malignant traits. GRP94 participates in ER quality control and can engage multiple downstream pathways, including PI3K/AKT, JNK, p38, NF-κB and Wnt/β-catenin, depending on its client proteins, such as TLRs, integrins, IGF-I/II and the Wnt co-receptor LRP6 (14-17,34,35,40,46-48). It is therefore possible that ERK/c-Myc downregulation in GRP94-deficient cells partly reflects a broader proteostatic and stress response rather than a single linear cascade. Similarly, the migration deficits observed after GRP94 knockdown may reflect changes in cell-surface composition downstream of its folding and trafficking functions. As aforementioned, a previous study has suggested a potential direct role of GRP94 in cell motility (45); however, whether comparable mechanisms operate in cervical cancer cells remains hypothetical and will require direct evaluation of cytoskeletal organization, integrin localization and migration under conditions that minimize proliferation-related confounding.

Kaplan-Meier analysis was further performed to explore the clinical significance of HSP90B1 upregulation using a public cervical cancer RNA-sequencing cohort. Using a median expression cut-off, the near-significant (P=0.073) results showed that high HSP90B1 expression was associated with a trend of poorer of overall survival. Although GRP94 was consistently upregulated in the paired clinical specimens and functionally supported proliferation and migration in cervical cancer cells, its value as a standalone prognostic marker remains unresolved. Larger clinical cohorts with standardized GRP94 protein-level assessment, detailed clinicopathological annotation, HPV subtype information, treatment history and long-term follow-up will be required to determine whether GRP94 has independent prognostic or therapeutic response relevance in cervical cancer.

These interpretive issues intersect with the main limitations of the present study. The current findings derive from *ex vivo* tissue and *in vitro* cell line investigations. The current study did not examine *in vivo* models of cervical cancer, and therefore, the impact of GRP94 modulation on tumor growth, invasion and therapeutic response in an intact microenvironment remains unknown. At the mechanistic level, the present study initially focused on ERK/c-Myc, and rescue or knockdown experiments were not performed to evaluate the necessity and sufficiency of these signaling pathways. The scope of the current study did not allow mapping of the upstream signaling proteins that link GRP94 to ERK maintenance in cervical cancer cells, leaving open which receptors or adhesion modules are most critical. Finally, the clinical cohort comprised 6 paired specimens without stratification by stage, HPV genotype or outcome, thus limiting the ability to assess whether GRP94 expression carries prognostic information or associates with other clinicopathological features in cervical cancer. The clinical association of GRP94 remains incompletely defined. Although an exploratory public database Kaplan-Meier analysis showed a trend toward poorer overall survival in patients with high HSP90B1 expression, the association did not reach statistical significance. Therefore, the prognostic value of GRP94 requires validation in larger, well-annotated cohorts. These constraints define the scope within which the present findings should be interpreted with caution.

In summary, across paired clinical specimens and two cervical cancer cell lines, it was found that GRP94 is upregulated in malignant cervical tissue, and that acute GRP94 suppression impairs cell proliferation and migration. These functional effects were accompanied by S-phase accumulation, decreased cyclin D1 and increased p21 levels, as well as reduced ERK and c-Myc levels, supporting a model in which GRP94 sustains cell proliferation and migration pathways in cervical cancer cells. Limited by the scope of the present

study together with the current knowledge on GRP94, the potential therapeutic implications should be interpreted cautiously, especially as the clinical development of pan-HSP90 inhibitors has been constrained by dose-limiting toxicity and limited therapeutic windows (48,49), whereas GRP94-selective inhibitors remain largely at the preclinical stage (50). Nevertheless, future studies should extend these findings to *in vivo* models, including subcutaneous or orthotopic cervical cancer xenografts, to determine whether GRP94 knockdown suppresses tumor growth, reduces ERK/c-Myc signaling in tumor tissues, and affects tumor cell proliferation or migration in a physiological microenvironment. *In vivo* studies using GRP94 knockdown or selective GRP94 inhibitors in cervical cancer models will be important to strengthen the physiological relevance of GRP94. Furthermore, experiments such as restoring ERK activity or c-Myc expression in GRP94-deficient cells and combining MEK inhibition with GRP94 knockdown, should clarify the extent to which the proliferation and migration phenotype of tumor cells is mediated through the ERK/c-Myc axis. Target mapping of GRP94-dependent receptors and adhesion complexes in cervical cancer, together with expanded clinical cohorts that integrate GRP94 expression with stage, HPV status and outcome, will help identify which GRP94-driven signaling pathways are most relevant in patients, and whether GRP94 or its downstream network merits consideration as a biomarker or therapeutic target.

**Acknowledgements**

The authors would like to thank the collaborator Dr Shuo Kang at Soochow University for carefully proofreading the manuscript.

**Funding**

The present study was supported by the Natural Science Foundation (grant no. 2022D01C469).

**Availability of data and materials**

The data generated in the present study may be requested from the corresponding author.

**Authors' contributions**

HT and ZA conceived and designed the study, and drafted the manuscript. HT, RA, YC and KD performed all experiments. YC and KD examined and analyzed raw image data. HT and ZA conducted statistical analysis. HT and ZA confirm the authenticity of all the raw data. All authors read and approved the final manuscript.

**Ethics approval and consent to participate**

The protocol of the present study, including human specimen collection and handling, was approved by The First Affiliated Hospital of Xinjiang Medical University Ethics Committee (approval no. 24030157). All participants provided written informed consent for participation in the study.

**Patient consent for publication**

Not applicable.

**Competing interests**

The authors declare that they have no competing interests.

**Use of artificial intelligence tools**

During the preparation of this work, artificial intelligence tools (ChatGPT5.1) were used to improve the readability and language of the manuscript or to generate images, and subsequently, the authors revised and edited the content produced by the artificial intelligence tools as necessary, taking full responsibility for the ultimate content of the present manuscript.

**References**

1. Arbyn M, Weiderpass E, Bruni L, de Sanjosé S, Saraiya M, Ferlay J and Bray F: Estimates of incidence and mortality of cervical cancer in 2018: A worldwide analysis. Lancet Glob Health 8: e191-e203, 2020.
2. Tang WZ, Cai QY, Huang KJ, Xu WZ, Li JZ, Pan YR, Xu HY, Zhao YF, Sheng TH, Li ZM, *et al*: The global burden of polycystic ovary syndrome, endometriosis, uterine fibroids, cervical cancer, uterine cancer, and ovarian cancer from 1990 to 2021. BMC Public Health 25: 1774, 2025.
3. Bray F, Laversanne M, Sung H, Ferlay J, Siegel RL, Soerjomataram I and Jemal A: Global cancer statistics 2022: GLOBOCAN estimates of incidence and mortality worldwide for 36 cancers in 185 countries. CA Cancer J Clin 74: 229-263, 2024.
4. Lu Y, Li P, Luo G, Liu D and Zou H: Cancer attributable to human papillomavirus infection in China: burden and trends. Cancer 126: 3719-3732, 2020.
5. Lorusso D, Xiang Y, Hasegawa K, Scambia G, Leiva M, Ramos-Elias P, Acevedo A, Sukhin V, Cloven N, Pereira de Santana Gomes AJ, *et al*: Pembrolizumab or placebo with chemoradiotherapy followed by pembrolizumab or placebo for newly diagnosed, high-risk, locally advanced cervical cancer (ENGOT-cx11/GOG-3047/KEYNOTE-A18): A randomised, double-blind, phase 3 trial. Lancet 403: 1341-1350, 2024.
6. Tewari KS and Monk BJ: Immunotherapy plus chemoradiotherapy in cervical cancer management. Lancet 403: 1310-1311, 2024.
7. Sharma S, Deep A and Sharma AK: Current treatment for cervical cancer: An update. Anticancer Agents Med Chem 20: 1768-1779, 2020.
8. Pal A and Kundu R: Human papillomavirus E6 and E7: The cervical cancer hallmarks and targets for therapy. Front Microbiol 10: 3116, 2020.
9. Hetz C, Zhang K and Kaufman RJ: Mechanisms, regulation and functions of the unfolded protein response. Nat Rev Mol Cell Biol 21: 421-438, 2020.
10. Biebl MM and Buchner J: Structure, function, and regulation of the Hsp90 machinery. Cold Spring Harb Perspect Biol 11: a034017, 2019.
11. Kim JW, Cho YB and Lee S: Cell surface GRP94 as a novel emerging therapeutic target for monoclonal antibody cancer therapy. Cells 10: 670, 2021.
12. Nomura H, Uzawa K, Yamano Y, Fushimi K, Ishigami T, Kato Y, Saito K, Nakashima D, Higo M, Kouzu Y, *et al*: Network-based analysis of calcium-binding protein genes identifies Grp94 as a target in human oral carcinogenesis. Br J Cancer 97: 792-801, 2007.
13. Hu T, Xie N, Qin C, Wang J and You Y: Glucose-regulated protein 94 is a novel glioma biomarker and promotes the aggressiveness of glioma via Wnt/β-catenin signaling pathway. Tumour Biol 36: 9357-9364, 2015.
14. Yang Y, Liu B, Dai J, Srivastava PK, Zammit DJ, Lefrançois L and Li Z: Heat shock protein gp96 is a master chaperone for toll-like receptors and is important in the innate function of macrophages. Immunity 26: 215-226, 2007.

15. Staron M, Yang Y, Liu B, Li J, Shen Y, Zúñiga-Pflücker JC, Aguila HL, Goldschneider I and Li Z: gp96, an endoplasmic reticulum master chaperone for integrins and Toll-like receptors, selectively regulates early T and B lymphopoiesis. Blood 115: 2380-2390, 2010.
16. Ostrovsky O, Ahmed NT and Argon Y: The chaperone activity of GRP94 toward insulin-like growth factor II is necessary for the stress response to serum deprivation. Mol Biol Cell 20: 1855-1864, 2009.
17. Liu B, Staron M, Hong F, Wu BX, Sun S, Morales C, Crosson CE, Tomlinson S, Kim I, Wu D and Li Z: Essential roles of grp94 in gut homeostasis via chaperoning canonical Wnt pathway. Proc Natl Acad Sci USA 110: 6877-6882, 2013.
18. Ajiro M and Zheng ZM: E6^E7, a novel splice isoform protein of human papillomavirus 16, stabilizes viral E6 and E7 oncoproteins via HSP90 and GRP78. mBio 6: e02068-14, 2015.
19. Chen X, Ding Y, Liu CG, Mikhail S and Yang CS: Overexpression of glucose-regulated protein 94 (Grp94) in esophageal adenocarcinomas of a rat surgical model and humans. Carcinogenesis 23: 123-130, 2002.
20. Wang Y and Wang X: A pan-cancer analysis of heat-shock protein 90 beta1(HSP90B1) in human tumours. Biomolecules 12: 1377, 2022.
21. Duan XF and Xin YW: Overexpression of molecule GRP94 favors tumor progression in lung adenocarcinoma by interaction with regulatory T cells. Thorac Cancer 11: 704-712, 2020.
22. Bouchard A, Sikner H, Baverel V, Garnier AR, Monterrat M, Moreau M, Limagne E, Garrido C, Kohli E, Collin B and Bellaye PS: The GRP94 inhibitor PU-WS13 decreases M2-like macrophages in murine TNBC tumors: A pharmaco-imaging study with 99mTc-Tilmanocept SPECT. Cells 10: 3393, 2021.
23. Dejeans N, Glorieux C, Guenin S, Beck R, Sid B, Rousseau R, Bisig B, Delvenne P, Buc Calderon P and Verrax J: Overexpression of GRP94 in breast cancer cells resistant to oxidative stress promotes high levels of cancer cell proliferation and migration: implications for tumor recurrence. Free Radic Biol Med 52: 993-1002, 2012.
24. Patel PD, Yan P, Seidler PM, Patel HJ, Sun W, Yang C, Que NS, Taldone T, Finotti P, Stephani RA, *et al*: Paralog-selective Hsp90 inhibitors define tumor-specific regulation of HER2. Nat Chem Biol 9: 677-684, 2013.
25. Song Q, Wen J, Li W, Xue J, Zhang Y, Liu H, Han J, Ning T and Lu Z: HSP90 promotes radioresistance of cervical cancer cells via reducing FBXO6-mediated CD147 polyubiquitination. Cancer Sci 113: 1463-1474, 2022.
26. Kubota H, Suzuki T, Lu J, Takahashi S, Sugita K, Sekiya S and Suzuki N: Increased expression of GRP94 protein is associated with decreased sensitivity to X-rays in cervical cancer cell lines. Int J Radiat Biol 81: 701-709, 2005.
27. Chang F, Steelman LS, Shelton JG, Lee JT, Navolanic PM, Blalock WL, Franklin R and McCubrey JA: Regulation of cell cycle progression and apoptosis by the Ras/Raf/MEK/ERK pathway (Review). Int J Oncol 22: 469-480, 2003.
28. García-Gutiérrez L, Delgado MD and León J: MYC oncogene contributions to release of cell cycle brakes. Genes (Basel) 10: 244, 2019.
29. Bhatla N, Aoki D, Sharma DN and Sankaranarayanan R: Cancer of the cervix uteri. Int J Gynaecol Obstet 143 (Suppl 2): S22-S36, 2018.
30. McShane LM, Altman DG, Sauerbrei W, Taube SE, Gion M and Clark GM; Statistics Subcommittee of the NCI-EORTC Working Group on Cancer Diagnostics: Reporting recommendations for tumor marker prognostic studies (REMARK). J Natl Cancer Inst 97: 1180-1184, 2005.
31. Livak KJ and Schmittgen TD: Analysis of relative gene expression data using real-time quantitative PCR and the 2(-Delta Delta C(T)) Method. Methods 25: 402-408, 2001.
32. Wersto RP, Chrest FJ, Leary JF, Morris C, Stetler-Stevenson MA and Gabrielson E: Doublet discrimination in DNA cell-cycle analysis. Cytometry 46: 296-306, 2001.
33. Watson JV, Chambers SH and Smith PJ: A pragmatic approach to the analysis of DNA histograms with a definable G1 peak. Cytometry 8: 1-8, 1987.
34. Batzorig U, Wei PL, Wang W, Huang CY and Chang YJ: Glucose-regulated protein 94 mediates the proliferation and metastasis through the regulation of ETV1 and MAPK pathway in colorectal cancer. Int J Med Sci 18: 2251-2261, 2021.
35. Wei PL, Huang CY, Tai CJ, Batzorig U, Cheng WL, Huang MT and Chang YJ: Glucose-regulated protein 94 mediates metastasis by CCT8 and the JNK pathway in hepatocellular carcinoma. Tumour Biol 37: 8219-8227, 2016.
36. Sears R, Nuckolls F, Haura E, Taya Y, Tamai K and Nevins JR: Multiple Ras-dependent phosphorylation pathways regulate Myc protein stability. Genes Dev 14: 2501-2514, 2000.
37. Marampon F, Ciccarelli C and Zani BM: Down-regulation of c-Myc following MEK/ERK inhibition halts the expression of malignant phenotype in rhabdomyosarcoma and in non muscle-derived human tumors. Mol Cancer 5: 31, 2006.
38. Wang Q, He Z, Zhang J, Wang Y, Wang T, Tong S, Wang L, Wang S and Chen Y: Overexpression of endoplasmic reticulum molecular chaperone GRP94 and GRP78 in human lung cancer tissues and its significance. Cancer Detect Prev 29: 544-551, 2005.
39. Langer R, Feith M, Siewert JR, Wester HJ and Hoefler H: Expression and clinical significance of glucose regulated proteins GRP78 (BiP) and GRP94 (GP96) in human adenocarcinomas of the esophagus. BMC Cancer 8: 70, 2008.
40. Huang CY, Lee CH, Tu CC, Wu CH, Huang MT, Wei PL and Chang YJ: Glucose-regulated protein 94 mediates progression and metastasis of esophageal squamous cell carcinoma via mitochondrial function and the NF-κB/COX-2/VEGF axis. Oncotarget 9: 9425-9441, 2018.
41. Pan Z, Erkan M, Streit S, Friess H and Kleeff J: Silencing of GRP94 expression promotes apoptosis in pancreatic cancer cells. Int J Oncol 35: 823-828, 2009.
42. Shen J, Yao L, Lin YG, DeMayo FJ, Lydon JP, Dubeau L and Lee AS: Glucose-regulated protein 94 deficiency induces squamous cell metaplasia and suppresses PTEN-null driven endometrial epithelial tumor development. Oncotarget 7: 14885-14897, 2016.
43. Chen WT, Tseng CC, Pfaffenbach K, Kanel G, Luo B, Stiles BL and Lee AS: Liver-specific knockout of GRP94 in mice disrupts cell adhesion, activates liver progenitor cells, and accelerates liver tumorigenesis. Hepatology 59: 947-957, 2014.
44. Luo B and Lee AS: The critical roles of endoplasmic reticulum chaperones and unfolded protein response in tumorigenesis and anticancer therapies. Oncogene 32: 805-818, 2013.
45. Ghosh S, Shinogle HE, Galeva NA, Dobrowsky RT and Blagg BS: Endoplasmic reticulum-resident heat shock protein 90 (HSP90) isoform glucose-regulated protein 94 (GRP94) regulates cell polarity and cancer cell migration by affecting intracellular transport. J Biol Chem 291: 8309-8323, 2016.
46. Wu S, Hong F, Gewirth D, Guo B, Liu B and Li Z: The molecular chaperone gp96/GRP94 interacts with Toll-like receptors and integrins via its C-terminal hydrophobic domain. J Biol Chem 287: 6735-6743, 2012.
47. Ansa-Addo EA, Thaxton J, Hong F, Wu BX, Zhang Y, Fugle CW, Metelli A, Riesenberg B, Williams K, Gewirth DT, *et al*: Clients and oncogenic roles of molecular chaperone gp96/grp94. Curr Top Med Chem 16: 2765-2778, 2016.
48. Liang X, Chen R, Wang C, Wang Y and Zhang J: Targeting HSP90 for cancer therapy: Current progress and emerging prospects. J Med Chem 67: 15968-15995, 2024.
49. Rastogi S, Joshi A, Sato N, Lee S, Lee MJ, Trepel JB and Neckers L: An update on the status of HSP90 inhibitors in cancer clinical trials. Cell Stress Chaperones 29: 519-539, 2024.
50. Pugh KW, Alnaed M, Brackett CM, and Blagg BSJ: The biology and inhibition of Grp94/gp96. Med Res Rev 42: 2007-2024, 2022.

Copyright © 2026 Tuerxun et al. This work is licensed under a Creative Commons Attribution-NonCommercial-NoDerivatives 4.0 International (CC BY-NC-ND 4.0) License.